Bioresource Technology 399 (2024) 130556

Contents lists available at ScienceDirect

Bioresource Technology

journal homepage: www.elsevier.com/locate/biortech

Biological carbon capture from biogas streams: Insights into *Cupriavidus necator* autotrophic growth and transcriptional profile

Rebecca Serna-García [a,1,*], Maria Silvia Morlino [b,1], Luca Bucci [b], Filippo Savio [b], Lorenzo Favaro [c,d], Tomas Morosinotto [b], Aurora Seco [a], Alberto Bouzas [a], Stefano Campanaro [b,2], Laura Treu [b,2]

[a] CALAGUA – Unidad Mixta UV-UPV, Department of Chemical Engineering, Universitat de València, Avinguda de la Universitat s/n, 46100 Burjassot, València, Spain
[b] Department of Biology, Università di Padova, Via U. Bassi 58/b, 35121, Padova, Italy
[c] Department of Agronomy, Food, Natural resources, Animals and Environment, Università di Padova, Viale dell'università 16, 35020, Legnaro, Italy
[d] Department of Microbiology, Stellenbosch University, Private Bag X1, Matieland 7602, South Africa

HIGHLIGHTS

- *Cupriavidus necator* can grow by consuming CO_2 derived from raw biogas streams.
- The choice of growth conditions is crucial for the setup of autotrophic cultivation.
- Biogas upgrading is achieved through the effective CO_2 assimilation by *C. necator*.
- Transcriptomics prove the relevance of inoculum adaptation for autotrophic growth.
- *C. necator* adapts to CO_2 changing the respiratory chain and central carbon metabolism.

GRAPHICAL ABSTRACT

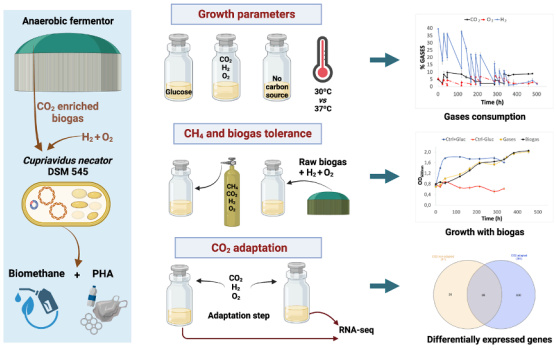

ARTICLE INFO

Keywords:
Biogas upgrading
Transcriptomics
Poly(3-hydroxybutyrate)
CO_2 capture
Cupriavidus necator

ABSTRACT

Recycling carbon-rich wastes into high-value platform chemicals through biological processes provides a sustainable alternative to petrochemicals. *Cupriavidus necator*, known for converting carbon dioxide (CO_2) into polyhydroxyalkanoates (PHA) was studied for the first time using biogas streams as the sole carbon source. The bacterium efficiently consumed biogenic CO_2 from raw biogas with methane at high concentrations (50%) proving non-toxic. Continuous addition of H_2 and O_2 enabled growth trends comparable to glucose-based heterotrophic growth. Transcriptomic analysis revealed CO_2-adaptated cultures exhibited upregulation of hydrogenases and Calvin cycle enzymes, as well as genes related to electron transport, nutrient uptake, and glyoxylate cycle. Non-adapted samples displayed activation of stress response mechanisms, suggesting potential lags in large-scale processes. These findings showcase the setting of growth parameters for a pioneering biological

* Corresponding author.
E-mail address: rebecca.serna@uv.es (R. Serna-García).
[1] These authors equally contributed to the work and shared first authorship.
[2] These authors equally contributed to the work and shared last authorship.

https://doi.org/10.1016/j.biortech.2024.130556
Received 17 January 2024; Received in revised form 25 February 2024; Accepted 6 March 2024
Available online 7 March 2024

biogas upgrading strategy, emphasizing the importance of inoculum adaptation for autotrophic growth and providing potential targets for genetic engineering to push PHA yields in future applications.

1. Introduction

Global warming and climate change are universally recognized to be mainly caused by greenhouse gas (GHG) emissions. Carbon dioxide (CO_2) stands out as one of the most prevalent GHGs produced through anthropic activities such as land use (including deforestation), which contributes for 10 % of total emissions, and fossil fuel consumption which contributes for 78 % (Friedlingstein et al., 2020). While reducing emissions is crucial, capturing and converting the generated CO_2 into valuable products via carbon capture and utilization (CCU) technologies is a fundamental complementary strategy for minimizing the environmental impact of industrial activities. CCU technologies are gaining significant attention for their potential to address climate change by treating CO_2 as a valuable resource, providing sustainable strategies for closing the carbon cycle and diminishing reliance on fossil fuels.

Biogas, derived from anaerobic fermentation of organic waste, consists of approximately 53–70 % CH_4, 30–47 % CO_2, and trace amounts of other gases (e.g., O_2, H_2O, N_2, H_2S, NH_3). Although the CO_2 present in biogas has a biological origin and does not contribute to a net increase in GHG emissions (Parravicini et al., 2022), it still holds potential for capture and recovery. Additionally, the high CO_2 percentages in raw biogas hamper combustion efficiency, restricting its utility to heat or electricity generation. CO_2 capture from biogas increases methane content (>95 % CH_4), potentially enabling direct injection of the biomethane obtained into gas grids or its use as a transport fuel. Hence, a process that captures CO_2 from biogas and converts it into valuable products would generate a dual value chain with a null or negative carbon balance.

Aerobic hydrogen-oxidizing bacteria (HOB) are facultative chemolithotrophs that can assimilate CO_2 through H_2 oxidation, utilizing fixed carbon for the synthesis of valuable products such as bioplastics or biofuels (Lin et al., 2022). *Cupriavidus necator* is a chemolithotrophic HOB that uses O_2 as an electron acceptor and H_2 as an electron donor for CO_2 uptake, fixing it via the Calvin-Benson-Bassham (CBB) cycle (Panich et al., 2021). This microorganism is known for its ability to store carbon reserves as polyhydroxyalkanoates (PHA), which are biocompatible and biodegradable polymers with plastic-like properties. Despite the potential of PHA to replace fossil-derived plastics, current obstacles revolve around their market prices, which heavily depend on the fermentation process and carbon sources of choice. Traditionally, PHA have been produced using pure cultures and expensive carbon sources, such as high-grade sugars or lipids, which approximately account for 30–50 % of the total production cost (Dalton et al., 2022). Further, economic competitiveness is hindered by the limited process yield and productivity (Kumar et al., 2020). The market price of PHA ranges from 2.4 to 5.5 US$ per kg, considerably higher than petroleum-based plastics (1.2 US$ per kg) (Crutchik et al., 2020). Hence, addressing the challenge of sustainable and competitive biological PHA production involves identifying cost-effective carbon sources, with CO_2 from biogas streams as an underexplored potential candidate.

C. necator has been proven to convert CO_2 into poly(3-hydroxybutyrate) (PHB), the most common homopolymeric PHA, albeit with limited yields due to low gas solubility in the liquid medium (Yu and Munasinghe, 2018) and the explosion risks related to oxyhydrogen cultivations (Lambauer and Kratzer, 2022). The last point is a significant process bottleneck, since H_2 - O_2 mixture management must be carried out on-site respecting the critical O_2 limit of 6.9 % v/v in the gas phase. In the first study on autotrophic PHB production, a biomass concentration of 91 g cell dry matter (CDM)/L and a PHB accumulation of 67 % were achieved, maintaining O_2 concentrations below 6.9 % (Tanaka et al., 1995). PHB accumulation in *C. necator* can reach up to 90 % of CDM under stress conditions such as limitation of nitrogen, phosphorus, or O_2 (Morlino et al., 2023; Koller, 2019). Taga et al. (1997) reported the highest documented PHB production from chemolithotrophic CO_2 fixation, reaching 82 % PHB content and a biomass accumulation of 60 g CDM/L. In that work, O_2 limitation stress was applied and an air-lift fermenter was employed to enhance gas–liquid mass transfer.

C. necator presents a versatile metabolism, capable of both heterotrophic and autotrophic growth, and mainly synthesizes PHB using acetyl-CoA as a precursor (Morlino et al., 2023). Although many articles debate PHB biosynthesis, the molecular mechanisms driving the shift from heterotrophy to chemolithotrophy, and particularly the relation between this shift and the regulation of PHB synthesis, are still underexplored. A proteomic study explored differences in protein abundance between chemolithotrophy and heterotrophy (Kohlmann et al., 2011). However, transcriptome analysis offers a more cost-effective means to comprehensively examine gene expression across diverse environmental conditions, enabling a thorough exploration of metabolic pathways and regulatory mechanisms, and providing potential targets for genetic engineering to optimize product yields (Jugder et al., 2015).

Although CO_2 conversion into PHB in *C. necator* is well-studied, direct utilization of CO_2 from raw biogas streams has never been tested. Specifically, information is lacking on the sensitivity of the bacterium to CH_4 or other gaseous anaerobic digestion byproducts. Furthermore, devising a biogas upgrading process involving *C. necator* requires assessing its capability to fix CO_2 in the presence of high percentages of CH_4. Few studies have investigated the shift from heterotrophic to chemolithotrophic metabolism in terms of growth, gas consumption or production, and the transcriptional regulation of the key genes involved. Understanding the bacterium's metabolic regulation is crucial for devising stable and efficient CO_2-to-PHA bioconversion strategies and achieving optimal yields. The current work aims at setting the groundwork for a combined process that allows the removal of a GHG and the simultaneous production of two value-added products: upgraded biomethane and PHA. Additionally, this research endeavors to integrate current knowledge on transcriptional changes underlying CO_2 fixation in *C. necator*.

2. Materials and methods

2.1. Organism, media, and nutrients

C. necator DSM 545, a mutant of *C. necator* DSM 529 that constitutively expresses glucose-6-phosphate dehydrogenase, being able to use glucose as carbon source, was supplied by the DSMZ collection (Deutsche Sammlung von Mikroorganismen und Zellkulturen, Braunschweig, Germany) and utilized for all experiments presented in this work. *C. necator* DSM 545 was maintained at −80 °C in a 25 % glycerol solution and activated, when needed, at ambient temperature in Nutrient Agar medium (peptone 5 g/L, yeast extract 2 g/L, NaCl 5 g/L, meat extract 1 g/L, agar 13 g/L). *C. necator* DSM 545 inoculum was grown at 30 °C under aerobic conditions in the mineral culture broth DSMZ 81 (DSMZ, Germany) using 0.5 L flasks. Information on DSMZ 81 medium composition can be found in Brojanigo et al. (2020). The final pH of the medium was around 6.9.

2.2. Experimental design and set-up

Different carbon sources, namely, glucose, pure CO_2, and biogas-derived CO_2, were used for testing *C. necator* growth rate. Pure gases were obtained from Sapio Produzione Idrogeno Ossigeno Srl (Milano,

Italy). Biogas was taken from the fermentor of the biogas plant Mirandola in Bovolone (Veneto, Italy), which treats agricultural residues. Biogas had a composition of 54 % CH_4 and 42 % CO_2.

Six experiments were performed to test metabolites and growth conditions (Table 1), including temperature comparison at 30 and 37 °C (Experiment 1), preferential utilization of glucose or CO_2 as the carbon source (Experiment 2), and gases (H_2, O_2, and CO_2) dynamics (Experiment 3). Experiment 4 assessed the impact of varying concentrations of CH_4 (10 or 50 %) on growth. In Experiment 5, the biological system was supplied with raw biogas for utilization of the biogas-derived CO_2 as a carbon source. Finally, Experiment 6 tested the effect of an adaptation period to CO_2 on autotrophic growth dynamics.

All the experimental setups started with a pre-inoculum which was cultivated aerobically on glucose in an Erlenmeyer flask. Subsequently, the pre-inoculum was inoculated at 10 % v/v in small-scale batch reactors, to investigate different conditions affecting biomass and PHA accumulation. Glucose leftovers in the medium from the pre-inoculum step allowed the bacterium to keep growing even after the inoculation in batches. Then, a negative control containing inoculum and DSMZ 81 medium, but no additional carbon source, was included to assess growth due to the residual glucose. A positive control with added glucose (5–10 $g{\cdot}L^{-1}$) was also included in all experiments to ensure reliable result interpretation. In Experiment 6, a CO_2 adaptation step was carried out in batches fed daily with a mixture of 40 %H_2:6%CO_2:5%O_2:49 %N_2 for seven days before performing the main experiment. This adaptation phase ensured complete consumption of residual glucose from the inoculum.

Experiments 1 to 3 were performed in 118 mL glass serum bottles with 40 mL working volume, while Experiments 4 to 6 employed 540 mL glass serum bottles with 180 mL working volume to increase the scale and cells amount. Bottles were sealed with rubber stoppers and aluminum crimps to avoid gas leakage. When needed, the bottles were flushed with different gases for 10 min to ensure the correct gas–liquid transfer, and then specific amounts of gases were added to the headspace through the rubber stoppers using graduate syringes (Table 1). In all experiments involving H_2 feeding, the O_2 percentage in the headspace was always kept below 6.9 %, to avoid any explosion risk (Lambauer and Kratzer, 2022). Bottle pressure was measured using a portable manometer (Delta Ohm HD2124.1, Italy). All bottles were incubated at the selected temperature under 150 rpm orbital shaking. The experiments were conducted in triplicates.

Table 1
Different conditions tested for *C. necator* growth.

Experiment	Bottle name	Pressure	Carbon source	Mixture of fed gases (%)	Gas flushed
Control bottles included in all experiments	Ctrl + gluc	1 atm	Glucose	–	Air
	Ctrl-gluc	1 atm	–	–	Air
1. Temperature comparison	Gases 37 °C	1.8 atm	CO_2	5 O_2; 40 H_2; 6 CO_2; 49 N_2	N_2
	Gases 30 °C	1.8 atm	CO_2	5 O_2; 40 H_2; 6 CO_2; 49 N_2	N_2
2. CO_2 /glucose growth	Gases	1 atm	CO_2	5 O_2; 40 H_2; 10 CO_2; 45 N_2	N_2
3. Gas consumption	Gases	1.8 atm	CO_2	5 O_2; 40 H_2; 5 CO_2; 50 N_2	N_2
4. Methane toxicity	Gases	2 atm	CO_2	5 O_2; 40 H_2; 5 CO_2; 50 N_2	N_2
	Gases + 10 % CH_4	2.2 atm	CO_2	5 O_2; 40 H_2; 5 CO_2; 10 CH_4; 40 N_2	N_2
	Gases + 50 % CH_4	2 atm	CO_2	5 O_2; 40 H_2; 5 CO_2; 50 CH_4	CH_4
5. Biogas test	Gases	2 atm	CO_2	5 O_2; 40 H_2; 5 CO_2; 50 N_2	N_2
	Biogas + H_2 + O_2	2 atm	CO_2 from biogas	5 O_2; 20 H_2; 31.5 CO_2; 3 N_2; 40.5 CH_4*	Biogas
	Biogas	1 atm	CO_2 from biogas	42 CO_2; 0.5 O_2; 54 CH_4 *	Biogas
6. CO_2 adaptation	CO_2 adapted	2 atm	CO_2	6.5 O_2; 40.5 H_2; 9.5 CO_2; 43.5 N_2	Air
	CO_2 not adapted	2 atm	CO_2	6.5 O_2; 40.5 H_2; 9.5 CO_2; 43.5 N_2	Air

*Presence of trace elements in values below 0.2%: hydrogen sulfide and hydrogen.

2.3. Analytical methods

Samples were regularly collected during 72–500 h of cultivation to track cell biomass concentration by measuring optical density (OD) and CDM. OD was determined by measuring the absorbance at 600 nm (OD_{600}) using a Spark® multimode microplate reader (Tecan, Switzerland). CDM was monitored gravimetrically by pelleting cells for 15 min at 4000 g and subsequently freezing the pellets at −20 °C and lyophilizing overnight.

Glucose concentration in cell-free supernatant (13,000 g for 4 min) was measured periodically with the Glucose Assay Kit (GAGO20, Sigma-Aldrich, USA) according to the manufacturer's instructions.

Gas was collected from the batch bottles' headspace using lock-tight syringes and its composition was analyzed by a gas chromatograph (8860 GC, Agilent Technologies, USA) equipped with a thermal conductivity detector (TCD). Three micropacked columns were used for the gas separation, namely Hayesep Q (1.5 m, 1/16″ OD, 1.0 mm ID), Hayesep N (0.5 m, 1/16″ OD, 1 mm ID), and MolSieve 5 Å (1.5 m, 1/16″ OD, 1.0 mm ID), all using helium (He) as carrier gas with a flow of 1.5 mL/min, at a pressure of 1.08 bar. Analyses were carried out at an oven temperature of 40 °C, and the TCD was set at 200 °C with a utility flow (He) of 15 mL/min and a makeup flow (He) of 5 mL/min. Gas volumes were calculated from gas compositions and normalized to conditions of 1 atm pressure and 0 °C temperature.

2.4. Polyhydroxyalkanoates extraction and analysis

The quantification of 3-hydroxybutyric acid (3HB) and 3-hydroxyvalerate acid (3HV) followed the method outlined in Torri et al. (2014) and Brojanigo et al. (2020), using gas chromatography with a Thermo Finnigan Trace GC equipped with a flame ionization detector (FID) and AT-WAX column (30 m, 0.25 mm, 0.25 μm). The gas carrier was He with a flow rate of 1.2 mL/min, and the split/splitless injector was set at 250 °C with a split ratio of 1:30. The FID and oven temperatures were set at 270 and 150 °C, respectively. Benzoic acid served as the internal standard, while 3HB, poly (3-hydroxybutyric acid-co-3-hydroxyvaleric acid), and P(3HB-co-14 mol% 3HV) were used as external standards, all obtained from Sigma-Aldrich (Milan, Italy). Results were expressed as percentages of PHB in CDM or grams of PHB per liter of culture.

2.5. RNA-seq and differential expression analysis

RNA sequencing was performed in Experiment 6 to evaluate the effect of CO_2 adaptation on the transcriptome of *C. necator*. For RNA extraction, 15 mL of culture were centrifuged at 4000 g for 10 min at 4 °C. Total RNA was extracted from the pellets with TRIzol™ reagent (Thermo Fisher Scientific, USA), according to the manufacturer's instructions. DNA contamination was removed by treating extracted RNA with DNase I, supplied with an RNA Clean & Concentrator™ kit (Zymo Research, USA). Samples were treated with the QIAseq FastSelect kit (Qiagen, USA) in order to mask ribosomal RNAs and maximize the

number of mRNA sequences. Subsequently, libraries were prepared with the Illumina Stranded mRNA Prep (Illumina Inc., USA) and sequencing was carried out on the Illumina Novaseq 6000 platform (2 × 150, paired-end) at the sequencing facility of the Department of Biology, University of Padua (https://www.biologia.unipd.it/dipartimento/organizzazione/settore-servizi-tecnici-alla-ricerca/ngs-facility/). In the transcriptomic analysis, reads were aligned on the reference genome sequence for *C. necator* H16 (RefSeq ID: GCF_000009285.2), given the accuracy of its annotation. RNA-seq Illumina paired-end reads were trimmed and filtered and gene counts were extracted from the alignment with the procedure described in Zampieri et al. (2023). Differential expression (DE) analysis was performed with DEseq2 (v. 3.14) (Love et al., 2014) by comparing CO_2-adapted and non-adapted cultures against glucose. Results were filtered by setting a threshold of 1 on the

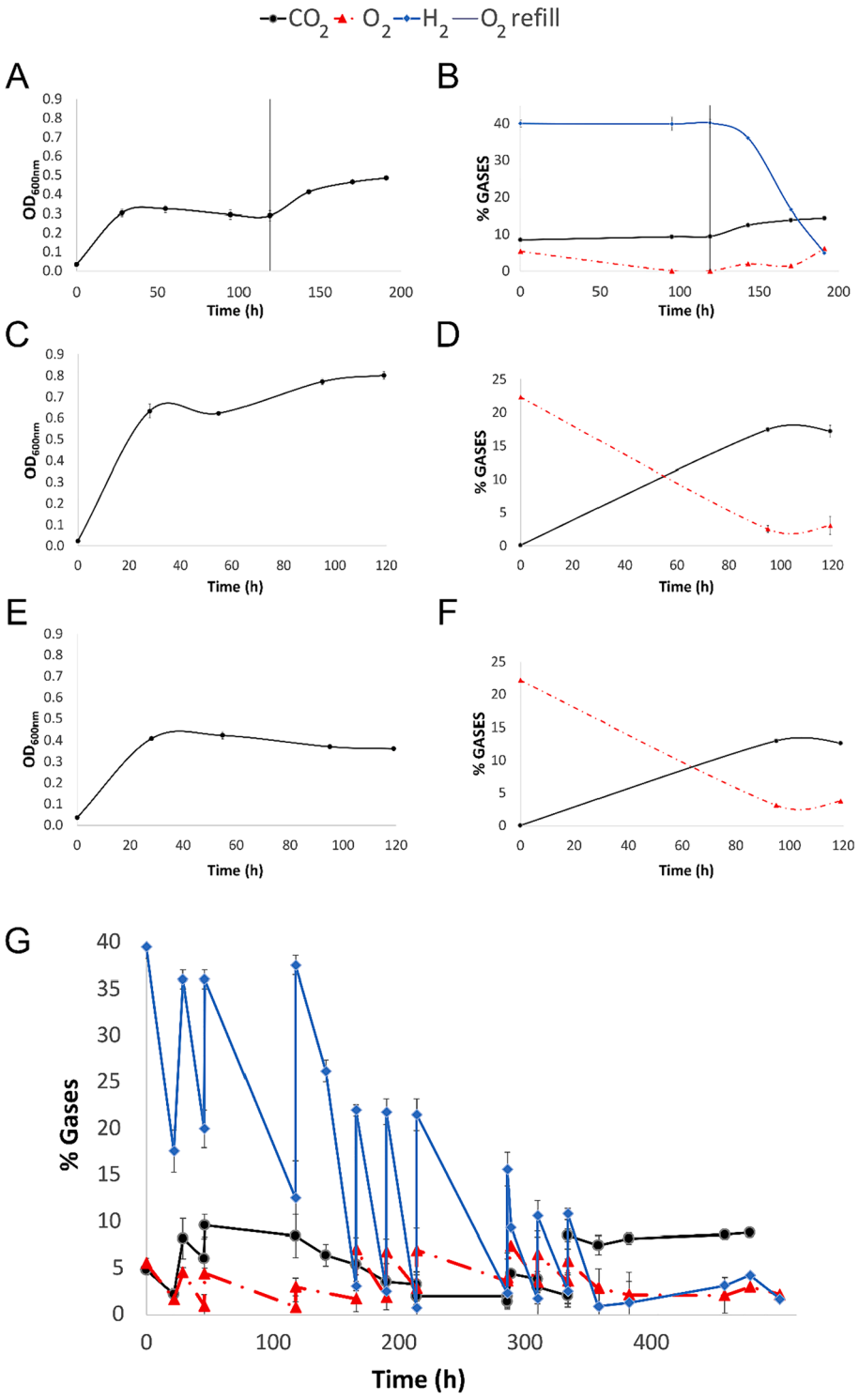

Fig. 1. Growth conditions assessment for *C. necator* DSM 545 on different carbon sources: glucose (Ctrl + Gluc) and a gas mixture including CO_2, H_2, and O_2. The negative control without an added carbon source (Ctrl-Gluc) is also reported. Data reported are the mean of three replicates (±SD). Panels **(a-f)** illustrate the evolution of OD_{600} and gases on different carbon sources in Experiment 2: CO_2 (a-b), glucose (10 $g{\cdot}L^{-1}$) (c-d), and residual glucose (4 $g{\cdot}L^{-1}$) from inoculum (e-f) without continuous gas refilling. In panel **(g),** gas consumption or production during H_2 and O_2 refilling in the culture in Experiment 3 is reported.

absolute log fold change (LFC). Benjamini-Hochberg correction for p-values was applied to each gene and the threshold for adjusted p-value (Q-value) was set at 0.05. Lists of significant differentially expressed genes (DEG) were generated for each comparison. Principal component analysis (PCA) was performed as implemented by DESeq2 using the 500 genes with the highest variance across samples. Gene annotation for *C. necator* H16 was retrieved from the Kyoto Encyclopedia of Genes and Genomes (KEGG) database (entry T00416).

3. Results and Discussion

3.1. Optimization of autotrophic growth conditions

A series of experiments was performed with the aim to assess optimal growth conditions and observe the dynamics of headspace gas concentrations under various conditions, with the main objective of characterizing autotrophic growth in batch mode. *C. necator* DSM 545 was grown at 30 and 37 °C in Experiment 1, according to the optimal temperature growth range of this mesophilic microorganism (Cavalheiro et al., 2009; Sheu et al., 2012; Sangkharak et al., 2021). Biomass accumulation was evaluated at both temperatures using glucose or CO_2 as the carbon source. Comparable OD_{600} values were obtained at both temperatures with glucose, while at 30 °C a higher OD_{600} was obtained when using CO_2 as carbon source (see supplementary material). This aligns with autotrophic growth studies typically conducted at 30 °C (Garcia-Gonzalez et al., 2015; Miyahara et al., 2022; Yu and Munasinghe, 2018). This trend is likely due to the influence of temperature on gas solubility in liquid: the lower the temperature, the higher the solubility of the gases fed (CO_2, H_2, O_2). A lag phase of approximately 300 h, during which no growth was detected, was observed while using CO_2 at 37 °C; in contrast, no lag phase was recorded at 30 °C. This is likely due to lower gas solubility at 37 °C, which may have resulted in a slowdown of microbial growth. Sheu et al. (2012) reported an absence of growth at 37 °C within a 48-hour timeframe, suggesting the presence of a lag phase phenomenon as well. According to these findings, all following experiments were performed at 30 °C.

Subsequently, the growth (OD_{600}) and dynamics of gases consumption and production were evaluated using alternatively CO_2 or glucose as carbon sources, and compared to a negative control with no added carbon source (Fig. 1a–f). O_2 was consistently consumed in the three sets of bottles, while glucose-grown bottles and negative controls produced CO_2 during glucose utilization (Eq. (1). Specifically, CO_2 headspace concentrations reached approximately 18 % in the bottles with added glucose (10 $g{\cdot}L^{-1}$), and around 14 % in negative controls that only contained residual glucose not consumed from the inoculum (4 $g{\cdot}L^{-1}$). Accordingly, in negative controls only residual growth occurred, as evidenced by the lower OD_{600}. Gas consumption trends of autotrophic bottles suggest that O_2 availability was a limiting factor for CO_2 and H_2 consumption. Indeed, upon reintroducing O_2 after 119 h, the microorganism resumed growth and H_2 uptake, although CO_2 consumption could not be detected (Fig. 1a, b). Analysis of accumulated PHA at the end of the experiment indicated that only PHB was produced. Bottles with glucose and negative controls accumulated up to 37 and 7 % of CDW, respectively, while PHB content reached up to 10 % in cultures growing on CO_2. (Mozumder, 2015)

$$C_6H_{12}O_6 + 1.97O_2 + 0.72NH_4^+ \Rightarrow 3.79CH_{1.74}O_{0.46}N_{0.19} + 2.21CO_2 + 0.7_2H^+ + 3.78H_2O \quad (1)$$

To address the issue of gas limitation, autotrophic cultures were set up and their daily gas consumption was monitored, replenishing H_2 and O_2 upon depletion. Once gas availability was no longer a growth-limiting factor, the microorganism initiated CO_2 uptake (Fig. 1g). In fact, the growth exceeded that observed in the previous experiment (Experiment 2), when O_2 was only refilled once, and was even higher than that observed in glucose-grown cultures.

In the subsequent trials (from Experiment 4 to 6), the volume of bottles was increased from 118 mL to 540 mL, and pressure was daily measured to precisely control the amount of gases being produced or consumed.

3.2. Assessment of growth with biogas

Pure CH_4 and real biogas were introduced in *C. necator* cultures to evaluate their effect on growth and gas dynamics (Table 1). *C. necator* DSM 545 growth was observed in both these conditions (Fig. 2). As expected, the exclusive feeding of biogas (42 % CO_2, 54 % CH_4) hindered growth, primarily because of the absence of O_2 as a suitable electron acceptor for respiration and ATP production (Cramm, 2009).

Results from Experiment 4 showed that CH_4 was not toxic to *C. necator* DSM 545, nor it was consumed, consistently with the known metabolic properties of the microorganism (Cramm, 2009). Similar biomass accumulation was achieved with 10 or 50 % CH_4 in the headspace. When 50 % CH_4 was provided, an initial lag phase was recorded, although the strain ultimately consumed CO_2 and achieved OD_{600} values similar to the other experimental conditions reported above (Fig. 2a). Once assessed that high CH_4 concentrations did not significantly impact growth, an experiment with real biogas was carried out in order to evaluate the effect of other trace compounds commonly present (Fig. 2b). Growth trends on biogas supplemented with H_2 and O_2 and on a H_2:CO_2:O_2:N_2 mixture were compared (Table 1). The growth profiles obtained in the two conditions were similar, and no detrimental effect was observed in the presence of raw biogas (Fig. 2b). This observation holds particular significance, considering that raw biogas contains other trace compounds, such as H_2S, which could potentially impact microbial growth. This finding is of great biotechnological interest, however, due to the high variability in biogas composition, it should be validated using biogas from different plants in order to reinforce these observations.

In both experiments, PHB content was measured after six days of growth. As expected, the lack of nutritional stress applied resulted in a low PHB accumulation, around 8–18 % CDW (Fig. 2c,d). However, it is worth noting that basal PHB accumulation remained comparable to autotrophic controls with no CH_4 in the headspace.

Taken together, these findings confirm the ability of *C. necator* DSM 545 to effectively utilize biogas as feedstock upon O_2 and H_2 supplementation. This promising result opens the door to a potential upscale of this process in a pilot setting, thereby enabling biogas upgrading. It is expected that the simultaneous removal of CO_2 present in biogas and the externally provided O_2 and H_2 obtained through environmentally friendly technologies can lead to successful and overall sustainable biomethane production. The H_2 required can be obtained through dark fermentation or water electrolysis, with a crucial consideration: the electricity used should exclusively derive from an excess of renewable energy sources such as photovoltaic or wind power plants. Integrating biogas upgrading with CO_2-to-PHB bioconversion enhances the positive environmental impact of the process by effectively implementing CO_2 utilization, thereby contributing to carbon neutrality or achieving negative emissions within the biogas sector. However, process optimization must entail a deep knowledge of the autotrophic metabolism of

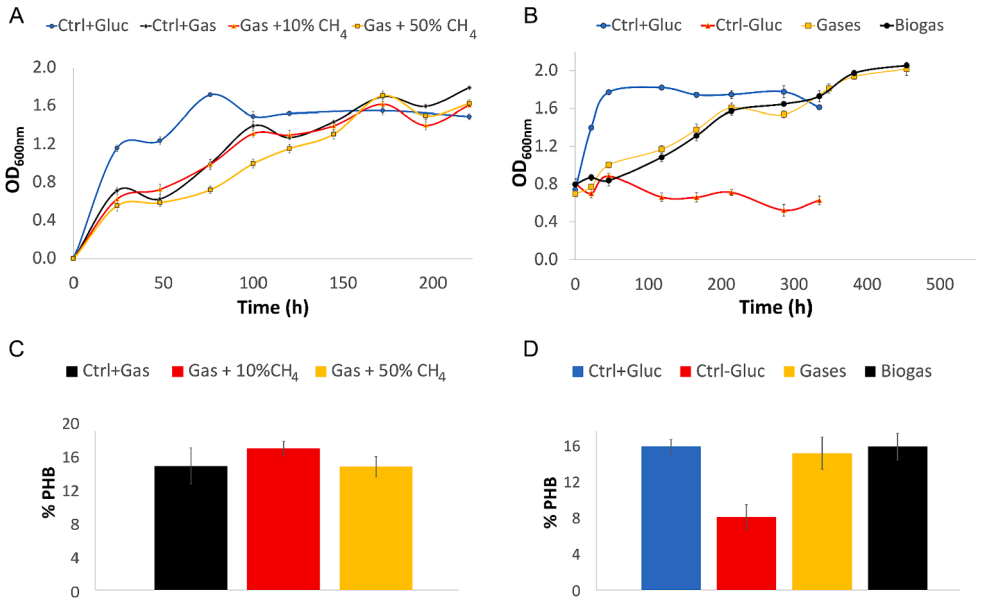

Fig. 2. Growth, OD_{600} (±SD), of *C. necator* DSM 545 in Experiment 4, assessing methane toxicity at two different concentrations of 10 and 50 % (**a**). Growth of *C. necator* recorded in experiment 5, in which biogas was used as a carbon source (**b**). Growth in the presence of methane or biogas is compared to that with the gas mixture prepared including CO_2, H_2 and O_2. The positive control with glucose (Ctrl + Gluc) and the negative control without an added carbon source (Ctrl-Gluc) are also included for reference. Polyhydroxybutyrate (PHB) accumulation after 6 days is shown in **(c)** and **(d)** for Experiments 4, and 5, respectively.

the organism, and whether it can be enhanced with prolonged periods of adaptation to CO_2. Indeed, a detailed transcriptional profile of autotrophic growth can help the identification of bottlenecks in the metabolism and the mechanisms of the organism's metabolic shifts. This knowledge can be exploited to fine-tune operational parameters, or devise genetic engineering strategies to boost PHA production from biogas.

3.3. Carbon dioxide adaptation process

A specific experiment was carried out to evaluate the effect of CO_2 adaptation on biomass growth, its consumption rate, and the transcriptional changes underlying CO_2 fixation. A comparison was made between a two-stage growth process, where the microorganism was initially grown heterotrophically and then shifted to autotrophic growth, and a single-stage process where the strain was directly cultivated autotrophically after undergoing some adaptation steps. The cultures were monitored over nine days, with daily assessments of their gas consumption and OD_{600} (Fig. 3). In the case of non-adapted *C. necator* DSM 545, an initial growth pattern resembling that of the control with glucose during the first 24 h was observed, presumably due to the consumption of residual glucose from the inoculum (Fig. 3a). However, apart from slightly lower hydrogen consumption in the first 24 h, no important differences in gas dynamics were observed between the two conditions tested, suggesting that adaptation does not enhance CO_2 uptake over time (Fig. 3b). Overall, non-adapted cultures show both fast growth from residual sugar and ready CO_2 consumption in the first 24 h, suggesting that their metabolic state is different from CO_2-adapted cultures.

An RNA-seq analysis was carried out to compare the three conditions of growth on glucose, CO_2 without previous adaptation, and CO_2 after one week of adaptation (Fig. 4). Glucose was used as a control to identify DEG in the two autotrophic conditions. Therefore, in the following paragraphs, DE values are always referred to the positive control with glucose. Positive LFC indicates that the genes have higher expression in the tested condition, while negative LFC indicates that the genes have higher expression in the control with glucose.

3.3.1. Transcriptional profile of carbon dioxide non-adapted samples

Transcriptomic analysis in the three conditions revealed distinct profiles (Fig. 4a), with major changes observed in CO_2-adapted samples (365 DEG) rather than CO_2 non-adapted samples (61 DEG) (Fig. 4b; see supplementary material). This discrepancy suggests that the presence of residual glucose in non-adapted samples delays the expression of genes associated with autotrophic metabolism, resulting in intermediate expression levels between glucose and CO_2-adapted conditions. Certain

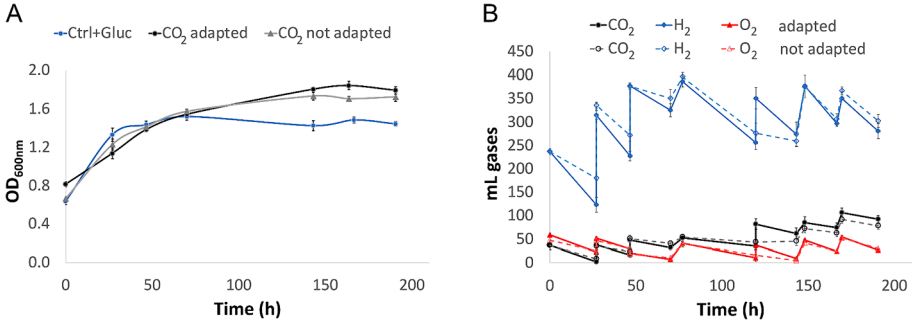

Fig. 3. Comparison of *C. necator* DSM 545 growth, OD_{600}, (**a**) and gases evolution (**b**) (±SD) for two tested conditions: CO_2-adapted and non-adapted cultures. A control with glucose (Ctrl + Gluc) is also included in (**a**) for comparison.

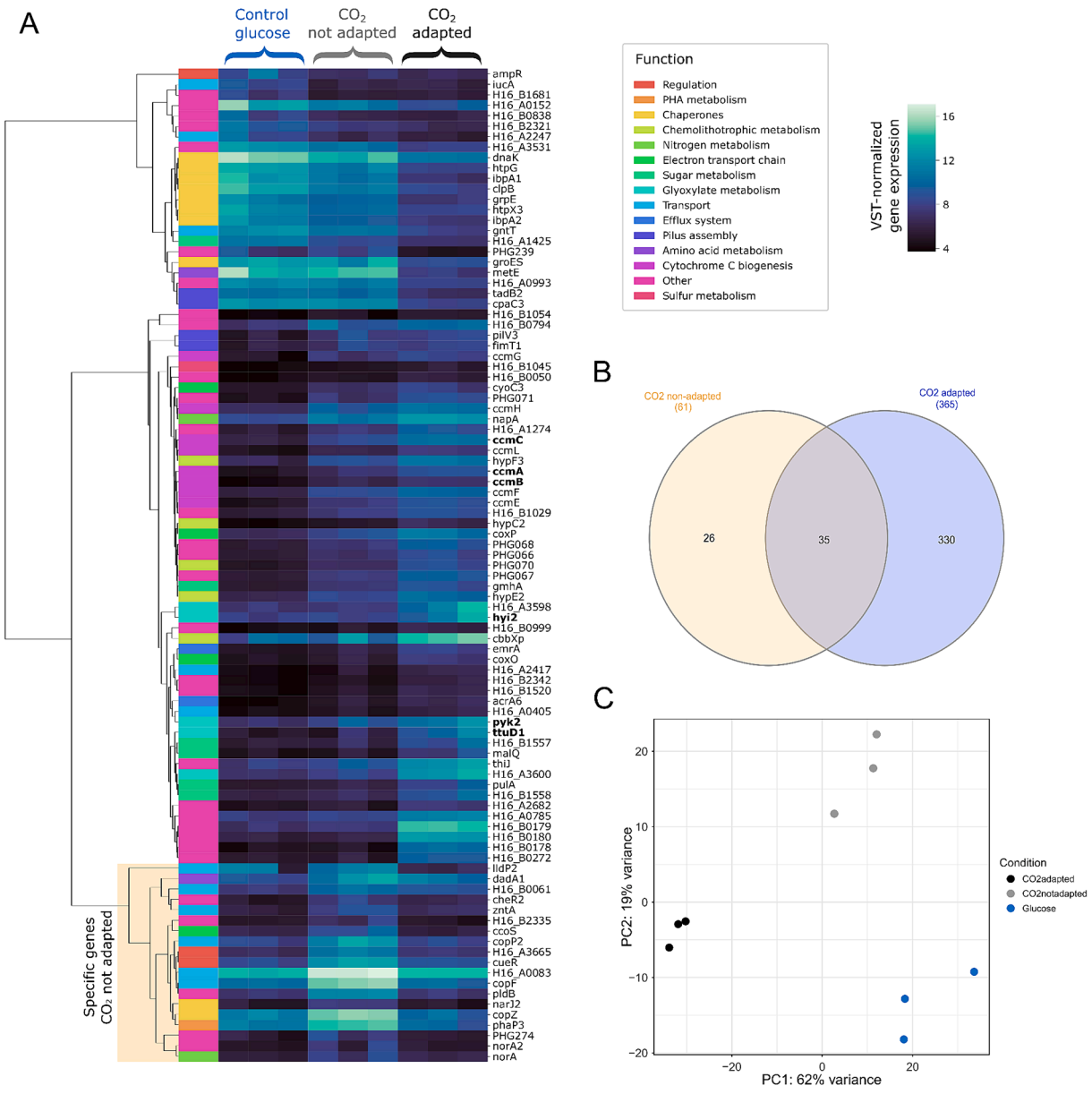

Fig. 4. Normalized expression of 95 significant, highly variable genes (absolute LFC > 3 in at least one comparison). Expression data are normalized by variance-stabilizing transformation. Genes are labeled by functional categories based on KEGG database annotations for *C. necator* H16 (**a**). Venn diagram of genes found as differentially expressed in CO_2 non-adapted and adapted samples (**b**). Principal component analysis of samples based on the expression values of the 500 most variable genes (**c**).

genes involved in hydrogenase expression and maturation, such as *hypD2*, *hypE2*, and *hypF3*, displayed this pattern, as well as the *ccm* operon, containing genes for cytochrome biogenesis and heme export (LFCs 2.8 to 5.7), which have a role in the electron transport chain remodeling. However, 25 DEG, mainly involved in copper, nitrogen, and sulfur metabolism, were exclusively overexpressed in CO_2 non-adapted samples (Fig. 4b). In confirmation of this, in the PCA plot of transcriptional profiles, CO_2 non-adapted samples form a distinct cluster, displaced from other conditions along the second principal component (Fig. 4c). Upregulated genes exclusive to the CO_2 non-adapted condition include copper transporters *cueR*, *copP2*, and *copZ* (LFCs 3.9 to 4.6), and chemotaxis-related genes *cheR2* and *cheA2Y2* (LFCs of 3.7 and 2.6, respectively). Enhanced copper import could be associated with the biosynthesis of additional respiratory chain enzymes to support autotrophic growth; on the other hand, the chemotaxis signaling cascade could be activated as a stress response mechanism due to the scarcity of glucose (He and Bauer, 2014). Remarkably, a significant increase in the expression of the phasin-coding gene *phaP3* (H16_A2172) was observed. Phasins are structural proteins that coat PHB granules (Pötter et al., 2002), and their upregulation could indicate a change in granule arrangement or size triggered by the change in nutrient availability (Nygaard et al., 2021). Renownedly, PHB accumulation is tightly linked to the cell's nutritional state and can serve as a redox valve (Koller, 2019). Importantly, however, in CO_2 non-adapted samples there are no significant changes in the expression of other genes for PHB synthesis or depolymerization. Overall, the CO_2 non-adapted samples display an intermediate metabolic state with distinct characteristics (Fig. 4c), where energy investments to scavenge the residual glucose are paralleled by early activation of genes related to electron transport chain rearrangement and hydrogenase maturation.

3.3.2. *Effects of carbon dioxide adaptation on energy metabolism*

After CO_2 adaptation, *C. necator* DSM 545 successfully transitions to an autotrophic growth, showing marked differences in transcriptional

profile compared to growth in glucose (Fig. 4a; see supplementary material). Notable changes include the upregulation of key genes associated with autotrophic metabolism, such as CBB cycle enzymes and hydrogenase-related genes. In addition, functions of DEG encompass ABC-type transporters, electron carriers, molecular chaperones, sigma factors, motility and adherence proteins, lipid A biosynthesis, and metabolism of carbon and various biomolecules. While some findings align with previous proteomic studies (Kohlmann et al., 2011, Schwartz et al., 2009), no transcriptomic investigations comparing autotrophic and heterotrophic metabolism are found in the literature. As such, this transcriptomic analysis provides a more comprehensive view and identifies additional pathways potentially involved in metabolic shifts. Autotrophy in *C. necator* is based on H_2 oxidation, which is carried out mainly by a membrane-bound hydrogenase (MBH) and a soluble hydrogenase (SH). Surprisingly, genes for MBH and SH did not show significant upregulation in CO_2-adapted samples, but several hydrogenase maturation genes were upregulated, with LFCs ranging from 3.2 to 6.6 (Fig. 5; see supplementary material). Furthermore, genes PHG064 and PHG065, which encode a high-affinity actinobacterial hydrogenase (AH) (Schäfer et al., 2013), were upregulated with an LFC of ~ 2.7 (Fig. 5). This hydrogenase is not able to sustain autotrophic growth alone, and its role in relation to other hydrogenases is unclear (Kleihues et al., 2000). The strong upregulation of AH in well-established autotrophic growth could be related to the limited H_2 solubility and low gas–liquid mass transfer efficiency under orbital shaking, making a high-affinity hydrogenase more effective (Miyahara et al., 2022). Investigating AH expression under exponential autotrophic growth could provide insights into its function and potential as a target for metabolic engineering.

Electrons harvested by hydrogenases are funneled to terminal oxidases in the process of energy conservation. *C. necator* is endowed with several cytochromes and eight terminal oxidases (comprehensively reviewed in Cramm, 2009), and it has been shown that the nutritional state significantly influences the composition of the terminal oxidases pool (Kohlmann et al., 2011). In CO_2-adapted samples, genes encoding cytochrome oxidase Cta are downregulated, while *cox* and *cco* operons are upregulated (Fig. 5). Most remarkably, quinol oxidase Cyo3 is upregulated with LFCs between 2 and 4 (*cyoA3*, *cyoB3*, *cyoC3*, *cyoD3*, Fig. 5; see supplementary material). Quinol oxidases transfer electrons directly from quinol to O_2. As the quinone pool receives electrons directly from MBH, it could be speculated that activation of the autotrophic metabolism directs more electrons toward the quinone pool and

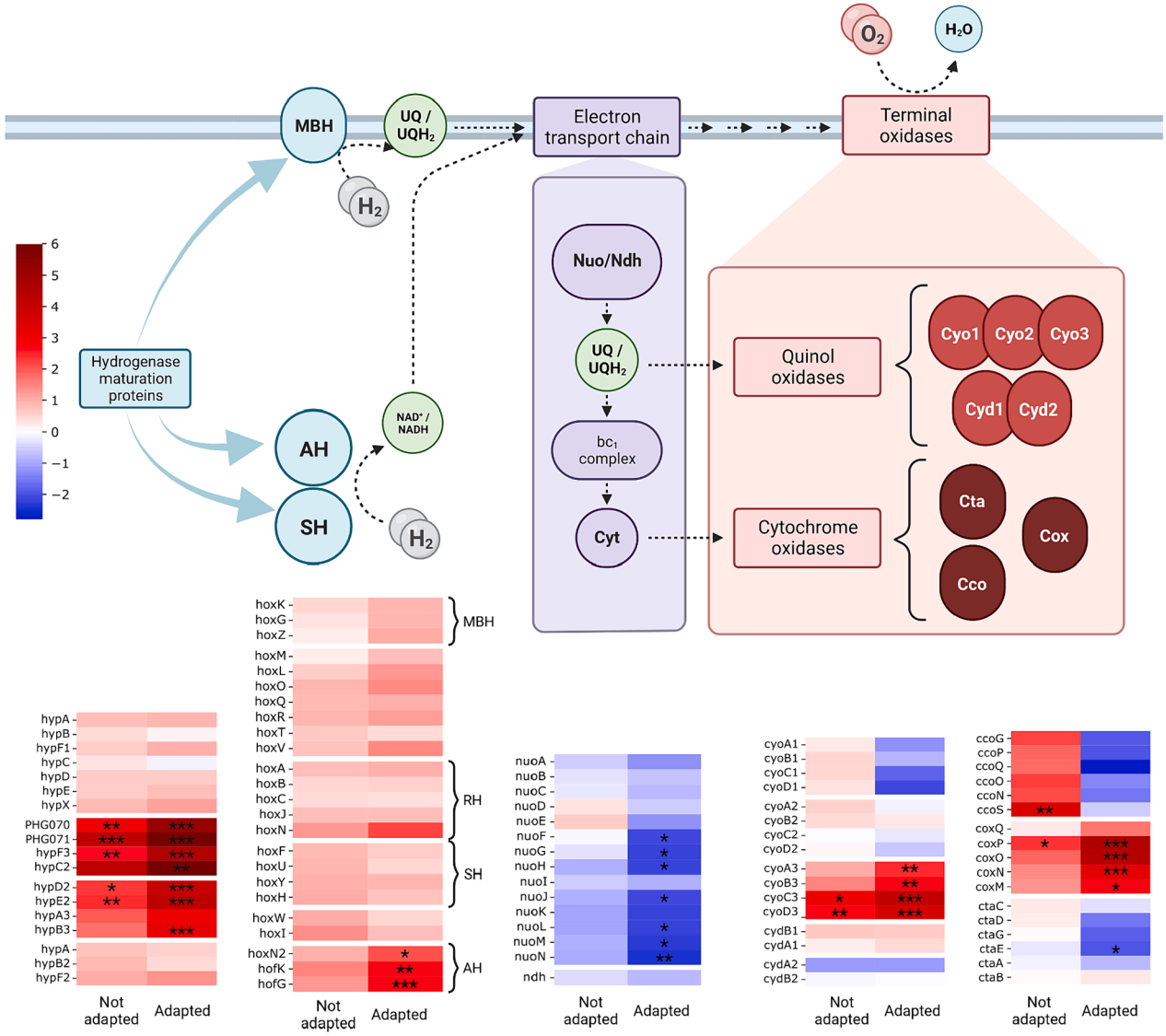

Fig. 5. Schematic view of autotrophic energy metabolism and variations in the expression of genes related to autotrophy. Significant variations are marked as follows: *, $q < 0.05$; **, $q < 10^{-3}$; ***, $q < 10^{-5}$. AH, actinobacterial hydrogenase; MBH, membrane-bound hydrogenase; Nuo and Ndh, NADH oxidoreductases; SH, soluble hydrogenase; UQ/UQH_2, ubiquinone/ubiquinol.

pushes quinol oxidase activity, bypassing cytochromes (Fig. 5). Supporting this hypothesis is the downregulation (LFC values ~ -2) of most genes encoding Nuo subunits, which receive electrons from SH in autotrophy. These observations align with the findings of a transcriptomic study where growth on glycerol was used to trigger hydrogenase derepression (Jugder et al., 2015). Overall, the changes brought to energy metabolism by autotrophic growth highlight the tight link between substrate utilization, electron flow, and hydrogenase expression. However, it must be noted that the energetic state of the cells in this experiment was likely limited by the culturing mode. Indeed, several genes involved in protein synthesis for ATPase assembly (see supplementary material), are downregulated, suggesting that ATP generation has decreased compared to heterotrophic samples. This may indicate that the adapted metabolism is slower overall. Notably, ATPase downregulation is not observed in non-adapted samples. Further transcriptional profiling of autotrophic samples in exponential growth, e.g. in a bioreactor, might clarify the relationship between expression of energy conservation-related genes and growth rate. Additionally, a thorough understanding of autotrophic energy metabolism could help maximize the accumulation of reducing power for CO_2 fixation. In particular, engineering the Nuo electron transport branch could be of special interest to influence NADH abundance in the cell, with potential consequences on carbon fixation and PHA production.

3.3.3. Changes in carbon and nutrient metabolism after carbon dioxide adaptation

The shift to autotrophic metabolism alters the requirements of inorganic compounds and key cofactors involved in energy conservation. Accordingly, CO_2-adapted samples display upregulation of ABC-type heme transporters. Genes encoding heme transporters are located on the pHG plasmid, in the *ccmABCDEFGH* operon, which encodes cytochrome *c* and accessory proteins for its maturation. Specifically, *ccmA*, *ccmB*, and *ccmC*, which have a crucial role in heme group binding, exhibit LFCs of 5.9, 6.8, and 5.1, respectively (Fig. 4a, Fig. 5).

Growth on different carbon sources determined changes in central carbon metabolism. Upregulation of RuBisCO subunits *cbbS2L2* on chromosome 2 and *cbbSpLp* on in plasmid pHG1, was observed (LFC values between 2.7 and 3.1). Lower glycolysis genes such as *pyk2*, *pyk3*, and *fbaB*, exhibit higher upregulation compared to the non-adapted condition (LFCs 4.8, 3.7, 2.3, respectively). The gene *pyk2* codes for pyruvate kinase and is part of a gene cluster (H16_A3598-602) involved in the glyoxylate cycle, which also exhibits upregulation (*hyi2*, LFC 4.7; *ttuD1*, LFC 6.6). This cycle facilitates the biosynthesis of carbohydrates from two-carbon molecules and aids chemolithoautotrophic growth by recycling the byproducts resulting from RuBisCO oxygenase activity (Claassens et al., 2020). Accordingly, phosphoglycolate phosphatase *cbbZ2*, catalyzing the first step of this conversion, was also upregulated (LFC 2.4). The glyoxylate cycle represents an excellent target for metabolic engineering to reduce acetate production and increase the production of derived molecules like 3-hydroxypropionate (Yang et al., 2022), which can serve as a precursor for PHA copolymers.

Autotrophic samples also displayed changes in genes involved in PHB metabolism. The gene H16_B2349, which codes for a sigma factor activator 54 involved in regulation of PHA synthesis (Hoffmann and Rehm, 2004; Rehm, 2006), was upregulated. In contrast, lower expression was observed for genes *phaA* and *phaB1*, which code for the enzymes catalyzing the first two steps of the PHA synthesis pathway. The activity of the PHA pathway is usually constant under stress-free conditions and increases in response to nutrient depletion (Morlino et al., 2023). It could be that the basal expression of the *phaC1AB1* operon is lower in lithoautotrophic conditions, potentially due to limited CO_2 transfer to the liquid phase, which could result in less carbon available to be routed to PHB accumulation.

The biochemical and transcriptomics results suggest a stepwise metabolic shift towards CO_2 adaptation. Genes such as hydrogenase and cytochrome maturation proteins are upregulated early (i.e., in CO_2 non-adapted samples), while other expression patterns appear at a later stage, with downregulation of Nuo and ATPase and upregulation of the CBB and glyoxylate shunt to support full-fledged autotrophic growth. Interestingly, upregulation of copper transporters occurs solely in CO_2 non-adapted samples, suggesting a temporary increase in copper demand related to a change in copper homeostasis upon the metabolic shift. Validation of these proposed mechanisms could be achieved through a time-series transcriptomic study. An important practical implication emerging from the results is that CO_2 adaptation would prove advantageous for effectively capturing CO_2 from gas streams. Although no notable physiological differences were observed on a small scale between CO_2-adapted or non-adapted cultures, the activation of various stress mechanisms was specifically observed in the non-adapted samples. When scaling up the process, CO_2 adaptation of the inoculum might make a significant difference in accelerating the initial growth stages, potentially leading to increased biomass concentration within shorter timeframes. This could facilitate an increase in the frequency of alternating cycles between biomass accumulation and stress induction, enhancing the potential for PHB accumulation on a larger scale.

4. Conclusions

This work provides key guidelines for *C. necator* cultivation start-up and demonstrates its ability to assimilate CO_2 from raw biogas, leading to GHG capture and subsequent biogas upgrading. The addition of H_2 and O_2 as electron donor and acceptor, respectively, was required for effective CO_2 uptake. Although this might initially dilute the treated biogas stream, these gasses are rapidly consumed, enabling effective upgrading. Transcriptomic analysis evidenced incomplete activation of autotrophic pathways in samples not adapted to CO_2. Thus, incorporating an adaptation period for biogas feeding might observably improve large-scale autotrophic implementation of this system.

Funding

This work was supported by ACT ERA-NET cofound under the European Union's Horizon 2020 Research and Innovation program (Project No 327,331 CooCE). This study was carried out within the MICS (Made in Italy – Circular and Sustainable) Extended Partnership and received funding from Next-GenerationEU (Italian PNRR – M4 C2, Invest 1.3 – D.D. 1551.11–10-2022, PE00000004). This work was also supported by the Spanish Ministry of Universities via a postdoctoral Margarita Salas (MS21-046) grant to the first author financed by the European Union (Next Generation EU).

Declaration of Generative AI and AI-assisted technologies in the writing process

During the preparation of this work the authors used ChatGPT in order to improve readability and language. After using this tool, the authors reviewed and edited the content as needed and take full responsibility for the content of the publication.

CRediT authorship contribution statement

Rebecca Serna-García: Writing – original draft, Visualization, Methodology, Investigation, Formal analysis, Conceptualization. **Maria Silvia Morlino:** Writing – original draft, Visualization, Investigation, Formal analysis, Data curation. **Luca Bucci:** Methodology, Investigation. **Filippo Savio:** Investigation, Formal analysis. **Lorenzo Favaro:** Writing – review & editing, Supervision, Resources. **Tomas Morosinotto:** Writing – review & editing, Project administration, Funding acquisition. **Aurora Seco:** Writing – review & editing, Supervision. **Alberto Bouzas:** Writing – review & editing, Supervision. **Stefano Campanaro:** Writing – review & editing, Supervision. **Laura Treu:** Writing – review & editing, Supervision, Funding acquisition.

Declaration of competing interest

The authors declare that they have no known competing financial interests or personal relationships that could have appeared to influence the work reported in this paper.

Data availability

Data will be made available on request.

Acknowledgments

The authors would like to gratefully acknowledge BTS Biogas (Affi, VR, Italy) for providing biogas samples from their plant. The authors wish to thank Sara Agostini (DAFNAE, University of Padova) for analytical and technical support in PHA quantification.

Appendix A. Supplementary data

Supplementary data to this article can be found online at https://doi.org/10.1016/j.biortech.2024.130556.

References

Brojanigo, S., Parro, E., Cazzorla, T., Favaro, L., Basaglia, M., Casella, S., 2020. Conversion of starchy waste streams into polyhydroxyalkanoates using *cupriavidus necator* DSM 545. Polymers. 12, 1496. https://doi.org/10.3390/polym12071496.

Cavalheiro JMBT, Almeida MCMD d, Grandfils C, Fonseca MMR., 2009. Poly(3-hydroxybutyrate) production by Cupriavidus necator using waste glycerol. Process Biochem. 44, 509–515. https://doi.org/10.1016/j.procbio.2009.01.008.

Claassens, N.J., Scarinci, G., Fischer, A., Bar-Even, A., 2020. Phosphoglycolate salvage in a chemolithoautotroph using the Calvin cycle. Biol. Sci. 117 (36), 22452–22461. https://doi.org/10.1073/pnas.2012288117.

Cramm, R., 2009. Genomic view of energy metabolism in *ralstonia eutropha* H16. MIP 16, 38–52. https://doi.org/10.1159/000142893.

Crutchik, D., Franchi, O., Caminos, L., Jeison, D., Belmonte, M., Pedrouso, A., Val del Rio, A., Mosquera-Corral, A., Campos, J.L., 2020. Polyhydroxyalkanoates (PHAs) production: a feasible economic option for the treatment of sewage sludge in municipal wastewater treatment plants. Water. 12, 1118. https://doi.org/10.3390/w12041118.

Dalton, B., Bhagabati, P., De Micco, J., Padamati, R.B., O'Connor, K., 2022. A review on biological synthesis of the biodegradable polymers polyhydroxyalkanoates and the development of multiple applications. Catalysts 12, 319. https://doi.org/10.3390/catal12030319.

Friedlingstein, P., et al., 2020. Global carbon budget 2020. Earth Sys. Sci. Data. 12 (4), 3269–3340. https://doi.org/10.5194/essd-12-3269-2020.

Garcia-Gonzalez, L., Mozumder, M.S.I., Dubreuil, M., Volcke, E.I.P., De Wever, H., 2015. Sustainable autotrophic production of polyhydroxybutyrate (PHB) from CO2 using a two-stage cultivation system. Catal. Today. 257 (2), 237–245. https://doi.org/10.1016/j.cattod.2014.05.025.

He, K., Bauer, C.E., 2014. Chemosensory signaling systems that control bacterial survival. Trends Microbiol 22, 389–398. https://doi.org/10.1016/j.tim.2014.04.004.

Hoffmann, N., Rehm, B.H.A., 2004. Regulation of polyhydroxyalkanoate biosynthesis in *pseudomonas putida* and *pseudomonas aeruginosa*. FEMS Microbiol. Lett. 237 (1), 1–7. https://doi.org/10.1016/j.femsle.2004.06.029.

Jugder, B.-E., Chen, Z., Ping, D.T.T., Lebhar, H., Welch, J., Marquis, C.P., 2015. An analysis of the changes in soluble hydrogenase and global gene expression in cupriavidus necator (ralstonia eutropha) H16 grown in heterotrophic diauxic batch culture. Microbial Cell Factories 14, 42. https://doi.org/10.1186/s12934-015-0226-4.

Kleihues, L., Lenz, O., Bernhard, M., Buhrke, T., Friedrich, B., 2000. The H2 sensor of ralstonia eutropha is a member of the subclass of regulatory [NiFe] hydrogenases. J Bacteriol 182, 2716–2724. https://doi.org/10.1128/jb.182.10.2716-2724.2000.

Kohlmann, Y., Pohlmann, A., Otto, A., Becher, D., Cramm, R., Lütte, S., Schwartz, E., Hecker, M., Friedrich, B., 2011. Analyses of soluble and membrane proteomes of *ralstonia eutropha* H16 reveal major changes in the protein complement in adaptation to lithoautotrophy. J Proteome Res. 10 (6), 2767–2776. https://doi.org/10.1021/pr101289v.

Koller, M., 2019. Chemical and biochemical engineering approaches in manufacturing polyhydroxyalkanoate (PHA) biopolyesters of tailored structure with focus on the diversity of building blocks. Chemical and Biochemical Engineering Quarterly 32, 413–438. https://doi.org/10.15255/CABEQ.2018.1385.

Kumar, M., Rathour, R., Singh, R., Sun, Y., Pandey, A., Gnansounou, E., Lin, K.Y.A., Tsang, D.C.W., Thakur, I.S., 2020. Bacterial polyhydroxyalkanoates: opportunities, challenges, and prospects. J. Clean. Prod. 263, 121500 https://doi.org/10.1016/j.jclepro.2020.121500.

Lambauer, V., Kratzer, R., 2022. Lab-scale cultivation of *cupriavidus necator* on explosive gas mixtures: carbon dioxide fixation into polyhydroxybutyrate. Bioengineering. 9, 204. https://doi.org/10.3390/bioengineering9050204.

Lin, L., Huang, H., Zhang, X., Dong, L., Chen, Y., 2022. Hydrogen-oxidizing bacteria and their applications in resource recovery and pollutant removal. Sci. Total. Environ. 835, 155559 https://doi.org/10.1016/j.scitotenv.2022.155559.

Love, M.I., Huber, W., Anders, S., 2014. Moderated estimation of fold change and dispersion for RNA-seq data with DESeq2. Genome Biol 15, 550. https://doi.org/10.1186/s13059-014-0550-8.

Miyahara, Y., Wang, C.-T., Ishii-Hyakutake, M., Tsuge, T., 2022. Continuous supply of non-combustible gas mixture for safe autotrophic culture to produce polyhydroxyalkanoate by hydrogen-oxidizing bacteria. Bioengineering. 9, 586. https://doi.org/10.3390/bioengineering9100586.

Morlino, M.S., Serna-García, R., Savio, F., Zampieri, G., Morosinotto, T., Treu, L., Campanaro, S., 2023. *Cupriavidus necator* as a platform for PHA production: an overview of strains, metabolism, and modeling approaches. Research Review Paper. Biotechnol. Adv. 108264 https://doi.org/10.1016/j.biotechadv.2023.108264.

Mozumder, M.S.I., 2015. In: Optimization of a Two-Phase Fermentation Process for the Production of Polyhydroxybutyrate (PHB) from Organic and Inorganic (industrial Waste) Substrate. Ghent University, Gent, Belgium, p. 198.

Nygaard, D., Yashchuk, O., Hermida, É.B., 2021. PHA granule formation and degradation by *cupriavidus necator* under different nutritional conditions. Journal of Basic Microbiology 61, 825–834. https://doi.org/10.1002/jobm.202100184.

Panich, J., Fong, B., Singer, S.W., 2021. Metabolic engineering of cupriavidus necator H16 for sustainable biofuels from CO_2. Trends Biotechnol. 39, 4. https://doi.org/10.1016/j.tibtech.2021.01.001.

Parravicini, V., Nielsen, P.H., Thornberg, D., Pistocchi, A., 2022. Evaluation of greenhouse gas emissions from the european urban wastewater sector, and options for their reduction. Sci. Total Environ. 838, 156322 https://doi.org/10.1016/j.scitotenv.2022.156322.

Pötter, M., Madkour, M.H., Mayer, F., Steinbüchel, A., 2002. Regulation of phasin expression and polyhydroxyalkanoate (PHA) granule formation in ralstonia eutropha H16. Microbiol 148 (8), 2413–2426. https://doi.org/10.1099/00221287-148-8-2413.

Rehm, B.H.A., 2006. Genetics and biochemistry of polyhydroxyalkanoate granule self-assembly: the key role of polyester synthases. Biotechnol. Lett. 28 (4), 207–213. https://doi.org/10.1007/s10529-005-5521-4.

Sangkharak, K., Paichid, N., Yunu, T., Klomklao, S., Prasertsan, P., 2021. Utilisation of tuna condensate waste from the canning industry as a novel substrate for polyhydroxyalkanoate production. Biomass Conv. Bioref. 11, 2053–2064. https://doi.org/10.1007/s13399-019-00581-4.

Schäfer, C., Friedrich, B., Lenz, O., 2013. Novel, oxygen-insensitive group 5 [NiFe]-hydrogenase in ralstonia eutropha. Applied and Environmental Microbiology 79, 5137–5145. https://doi.org/10.1128/AEM.01576-13.

Schwartz, E., Voigt, B., Zühlke, D., Pohlmann, A., Lenz, O., Albrecht, D., Schwarze, A., Kohlmann, Y., Krause, C., Hecker, M., Friedrich, B., 2009. A proteomic view of the facultatively chemolithoautotrophic lifestyle of *ralstonia eutropha* H16. PROTEOMICS 9, 5132–5142. https://doi.org/10.1002/pmic.200900333.

Sheu, D.S., Chen, W.M., Lai, Y.W., Chang, R.C., 2012. Mutations derived from the thermophilic polyhydroxyalkanoate synthase PhaC enhance the thermostability and activity of PhaC from *cupriavidus necator* H16. J Bacteriol. 194 (10), 2620–2629. https://doi.org/10.1128/JB.06543-11.

Taga, N., Tanaka, K., Ishizaki, A., 1997. Effects of rheological change by addition of carboxymethylcellulose in culture media of an air-lift fermentor on poly-d-3-hydroxybutyric acid productivity in autotrophic culture of hydrogen-oxidizing bacterium, Alcaligenes eutrophus. Biotechnol. Bioeng. 53, 529–533. https://doi.org/10.1002/(SICI)1097-0290(19970305)53:5<529::AID-BIT11>3.0.CO;2-B.

Tanaka, K., Ishizaki, A., Kanamaru, T., Kawano, T., 1995. Production of poly(D-3-hydroxybutyrate) from CO2, H2, and O2 by high cell density autotrophic cultivation of Alcaligenes eutrophus. Biotechnol. Bioeng. 45, 268–275. https://doi.org/10.1002/bit.260450312.

Torri, C., Cordiani, H., Samorì, C., Favaro, L., Fabbri, D., 2014. Fast procedure for the analysis of poly(hydroxyalkanoates) in bacterial cells by online pyrolysis/gas-chromatography with flame ionization detector. J. Chromatogr. A 1359, 230–236. https://doi.org/10.1016/j.chroma.2014.07.008.

Yang, P., Liu, W., Chen, Y., Gong, A.D., 2022. Engineering the glyoxylate cycle for chemical bioproduction. Front. Bioeng. Biotechnol. 10 https://doi.org/10.3389/fbioe.2022.1066651.

Yu, J., Munasinghe, P., 2018. Gas fermentation enhancement for chemolithotrophic growth of *cupriavidus necator* on carbon dioxide. Fermentation. 4, 63. https://doi.org/10.3390/fermentation4030063.

Zampieri, G., Campanaro, S., Angione, C., Treu, L., 2023. Metatranscriptomics-guided genome-scale metabolic modeling of microbial communities. Cell. Rep. Methods. 3 (1), 100383 https://doi.org/10.1016/j.crmeth.2022.10038.